This article was downloaded by: [University of Ottawa]
On: 11 June 2015, At: 01:45
Publisher: Taylor & Francis
Informa Ltd Registered in England and Wales Registered Number: 1072954 Registered office: Mortimer House, 37-41 Mortimer Street, London W1T 3JH, UK

Journal of Thermal Stresses
Publication details, including instructions for authors and subscription information:
http://www.tandfonline.com/loi/uths20

A Constitutive Equation of Thermoelasticity for Solid Materials

Q. H. Tang [a] , X. L. Liu [a] , C. Chen [a] & T. C. Wang [a]
[a] State Key Laboratory of Nonlinear Mechanics, Institute of Mechanics , Chinese Academy of Sciences , Beijing , China
Published online: 21 Apr 2015.

Click for updates

To cite this article: Q. H. Tang , X. L. Liu , C. Chen & T. C. Wang (2015) A Constitutive Equation of Thermoelasticity for Solid Materials, Journal of Thermal Stresses, 38:4, 359-376, DOI: 10.1080/01495739.2014.985556

To link to this article: http://dx.doi.org/10.1080/01495739.2014.985556

PLEASE SCROLL DOWN FOR ARTICLE

Taylor & Francis makes every effort to ensure the accuracy of all the information (the "Content") contained in the publications on our platform. However, Taylor & Francis, our agents, and our licensors make no representations or warranties whatsoever as to the accuracy, completeness, or suitability for any purpose of the Content. Any opinions and views expressed in this publication are the opinions and views of the authors, and are not the views of or endorsed by Taylor & Francis. The accuracy of the Content should not be relied upon and should be independently verified with primary sources of information. Taylor and Francis shall not be liable for any losses, actions, claims, proceedings, demands, costs, expenses, damages, and other liabilities whatsoever or howsoever caused arising directly or indirectly in connection with, in relation to or arising out of the use of the Content.

This article may be used for research, teaching, and private study purposes. Any substantial or systematic reproduction, redistribution, reselling, loan, sub-licensing, systematic supply, or distribution in any form to anyone is expressly forbidden. Terms & Conditions of access and use can be found at http://www.tandfonline.com/page/terms-and-conditions

Journal of Thermal Stresses, 38: 359–376, 2015
Copyright © Taylor & Francis Group, LLC
ISSN: 0149-5739 print/1521-074X online
DOI: 10.1080/01495739.2014.985556

Taylor & Francis
Taylor & Francis Group

A CONSTITUTIVE EQUATION OF THERMOELASTICITY FOR SOLID MATERIALS

Q. H. Tang, X. L. Liu, C. Chen, and T. C. Wang
State Key Laboratory of Nonlinear Mechanics, Institute of Mechanics, Chinese Academy of Sciences, Beijing, China

A new constitutive equation of thermoelasticity for crystals is presented based on the interatomic potential and solid mechanics at finite temperature. Using the new constitutive equation, the calculations for crystal copper and graphene are carried out under different loading paths at different temperatures. The calculated results are in good agreement with those of the previous thermoelasticity constitutive equation based on quantum mechanics, which clearly indicates that our new constitutive equation of thermoelasticity is correct. A lot of comparisons also show that the present theory is more concise and efficient than the previous thermal stress theory in the practical application.

Keywords: Constitutive equation; Finite temperature; Interatomic potential; Thermal stress theory

Downloaded by [University of Ottawa] at 01:45 11 June 2015

INTRODUCTION

Rapid progress in the synthesis and processing of materials with structure on tiny length scales has created a demand for greater scientific understanding of thermal behavior in microscale devices and nanostructured materials [1].

A lot of experiments on the thermal properties of materials have been performed. Some important experimental results were obtained, such as elastic constants [2, 3], heat capacity [4], the specific heat and coefficient of thermal expansion [4, 5] for Al, Au, Cu, diamond and graphene [6] at different temperatures. Moreover, anisotropic thermo-mechanical response of Ti–6Al–4V at various temperatures from 233 to 755 K has been studied by considering the complicated deformation behavior of materials [7, 8].

While describing thermal phenomena in different manners [9, 10], both atomistic and continuum models should be considered when considering theoretical investigations for the thermal properties of materials. In atomistic models, the total atomic motion consists of structural deformation and thermal vibration. Finite temperature effects in molecular dynamics simulations are accounted for

Received 1 April 2014; accepted 8 July 2014.
Address correspondence to T. C. Wang, State Key Laboratory of Nonlinear Mechanics, Institute of Mechanics, Chinese Academy of Sciences, No. 15 Beisihuanxi Road, Beijing 100190, PR China. E-mail: tcwang@imech.ac.cn

Color versions of one or more of the figures in the article can be found online at www.tandfonline.com/uths.

by combining atom velocity with environment temperature of available heat bath such as Andersen thermostat, Nose–Hoover thermostat, and the phonon heat bath method [11–13]. In continuum models, structural deformation and thermal vibration are treated separately. While the structural deformation part is explicitly modeled at the continuum level, the thermal oscillation of atoms in the material can only be expressed in the phenomenological form of heat energy.

To capture the essential features of atomistic physics while retaining the efficiency of continuum models, many multiscale methods and atomistic-based continuum theories have been proposed [14–17]. Tadmor et al. [18, 19], Shenoy et al. [20] and Tadmor and Miller [21] developed the quasicontinuum (QC) method by combining continuum finite element method with atomistic physics. The quasicontinuum (QC) method has played an important role to study the fracture. The QC method was extended to take into account the effect of finite temperature under local quasiharmonic approximation [22–24]. Shenoy et al. [22] presented a derivation of an effective energy function to perform Monte Carlo simulation in a mixed atomistic and continuum setting, namely QC Monte Carlo (QCMC) method.

Tang and Aluru [25] established a multiscale model based on finite element method for mechanical analysis of silicon nanostructures at finite temperature. Within the framework of local quasiharmonic model, Jiang et al. [9] studied bulk thermodynamic properties of graphite and diamond using their finite-temperature continuum theory developed in terms of the interatomic potential. Tang and Aluru [25] and Tang et al. [26] investigated three quasiharmonic models, namely QHM (quasiharmonic model), QHMK (quasiharmonic model in reciprocal space) and LQHM (local quasiharmonic model). The results reveal that LQHM does not accurately describe the thermal properties as it neglects the vibration coupling of the atoms.

Tadmor and Miller [21] pointed out that "the great disparity in scale and the interdisciplinary nature of the field are what makes modeling materials both challenging and exciting. There is increased awareness that materials must be understood, not only by rigorous treatment of phenomena at each of these scales alone, but rather through consideration of the interactions between theses scales. This is the paradigm of multiscale modeling. Materials modeling is, at its core, an endeavor to develop constitutive laws through a detailed understanding of these microstructural features, and this requires the observation and modeling of material at each of these different scales."

The objective of this article is to establish a new constitutive equation of thermoelasticity for crystals at finite temperature based on the interatomic potential and solid mechanics. This article is divided into four sections. The concept of thermal strain is introduced and the new constitutive relation is presented, followed by the results, discussion and conclusion. Some calculations of physical quantities are given in Appendices A and B.

CONSTITUTIVE EQUATION OF THERMOELASTICITY

The previous constitutive relation of thermal stress is reviewed next, and then the concept of thermal strain is introduced and a new constitutive equation of thermoelasticity is established, respectively.

Downloaded by [University of Ottawa] at 01:45 11 June 2015

THE PREVIOUS CONSTITUTIVE RELATION

A common characteristic of the previous proposed constitutive relations of thermal stress is based on the Helmholtz free energy function and the atomic interaction potential [9, 26, 27]. The Helmholtz free energy A can be expressed as [28]

$$A = U_{tot} + k_B T \sum_{i=1}^{3N} \ln[2\sinh(\frac{1}{2}\beta\hbar\omega_i)], \qquad \beta = 1/k_B T \tag{1}$$

Based on the Cauchy-Born rule [29], the continuum deformation can be related to the motion of atoms in the continuum, and the strain energy at the continuum level can be calculated by the energy stored in atomic bonds.

The first term U_{tot} in Eq. (1) describes the mechanical deformation under the applied load, the second term in Eq. (1) is the entropy of system, which describes the effect of temperature on the system deformation. The Cauchy–Born rule also indicates that atoms subjected to a homogeneous deformation move according to a single mapping from the undeformed to deformed configurations. Such a mapping is characterized by the continuum deformation gradient $\mathbf{F}$ of a material point which represents the collective behavior of many atoms that undergo locally uniform deformation. The Green strain tensor $\mathbf{E}$ can be expressed as

$$\mathbf{E} = (\mathbf{F}^T\mathbf{F} - \mathbf{I})/2 \tag{2}$$

According to the theory of solid mechanics, the second Piola–Kirchhoff stress $\mathbf{S}$ [9, 25, 30] are determined by

$$\mathbf{S} = \frac{1}{V_0}\frac{\partial A}{\partial \mathbf{E}} = \left\{\frac{\partial U_{tot}}{\partial \mathbf{E}} + \sum_i \frac{\overline{E}_i}{\omega_i}\cdot\frac{\partial \omega_i}{\partial \mathbf{E}}\right\}/V_0 \tag{3}$$

$$\overline{E_i} = \sum_i \left(\frac{1}{2}\hbar\omega_i + \frac{\hbar\omega_i}{e^{\hbar\omega_i/k_B T} - 1}\right) \tag{4}$$

The Cauchy stress $\boldsymbol{\sigma}$ can be expressed by

$$\boldsymbol{\sigma} = \mathbf{F}\{\frac{\partial U_{tot}}{\partial \mathbf{E}} + \sum_i \frac{\overline{E_i}}{\omega_i}\cdot\frac{\partial \omega_i}{\partial \mathbf{E}}\}\mathbf{F}^T/V \tag{5}$$

The vibration frequency ω_i and its derivative $\frac{\partial \omega_i}{\partial \mathbf{E}}$ are dependent on the interatomic potential and the strain tensor $\mathbf{E}$. Eq. (5) is the previous established constitutive relation based on the quantum mechanics due to the quantization of thermal energy $\overline{E}_i$.

By applying for the thermal stress theory Eq. (5), some researchers calculated the frequency ω_i of graphene and diamond via the local harmonic model [9], the frequency ω_i of silicon via the k-space quasiharmonic model [25], and the frequency ω_i of metal copper via the periodic boundary condition [31, 32]. These valuable works promote the development and application of the thermal stress theory.

Downloaded by [University of Ottawa] at 01:45 11 June 2015

THERMAL STRAIN CALCULATION METHODS

Before the new thermoelasticity constitutive relation is proposed, a concept of thermal strain is introduced. As an undeformed body without any constraint is heated from temperature T_0 to T, it should be expanding freely, and the strain caused by temperature change is called the thermal strain. The two methods of calculating the thermal strain are given as follows.

In Method 1, the thermal strain is given by

$$\varepsilon_T = \int_{T_0}^{T} \alpha dT \tag{6}$$

where T_0 is chosen to be room temperature, ε_T is the thermal strain from temperature T_0 to temperature T when the crystal is thermally expanding freely, α is the coefficient of thermal expansion (CTE). The detail calculation for α of copper is presented in Appendix A.

In Method 2, the lattice constant, $r^{(0)}(T)$, is determined by minimizing the Helmholtz free energy A.

$$\frac{\partial A}{\partial V} = 0 \tag{7}$$

Thermal strain can be expressed [9] by

$$\varepsilon_T = \frac{r^{(0)}(T)}{r^{(0)}(293K)} - 1 \tag{8}$$

where $r^{(0)}(T)$ is the equilibrium bond length at temperature T, $r^{(0)}(293\,K)$ is the equilibrium bond length at room temperature $T_0 = 293\,K$. The detail calculation for $r^{(0)}(T)$ of graphene is presented in Appendix B.

The comparison of the calculated results and experimental data [5] for thermal strain of copper is shown in Figure 1, both methods give fairly accurate results within the range of 800 K temperature. The thermal strain for graphene could be obtained by similar methods.

THE NEW STRESS-STRAIN RELATIONSHIP

The characteristic of new theory is based on the thermal strain and the large deformation theory instead of the Helmholtz free energy function, which make it more convenient in practical application than the previous theories. The effect of temperature on the mechanical behavior of materials is frequently crucial, and the physical phenomenon of coupling effect of thermal and mechanical is complicated. A lot of studies have been carried out in the past years by using the methods of experiment and theoretical analysis [5, 9]. As a crystal material is subjected to the external load at the finite temperature, its deformation should include both the mechanical deformation due to the external load and thermal deformation due to temperature. Therefore the total deformation of a crystal should be a superposition of the elastic deformation and the thermal deformation due to the thermal vibration of the atoms around the crystal lattice.

Downloaded by [University of Ottawa] at 01:45 11 June 2015

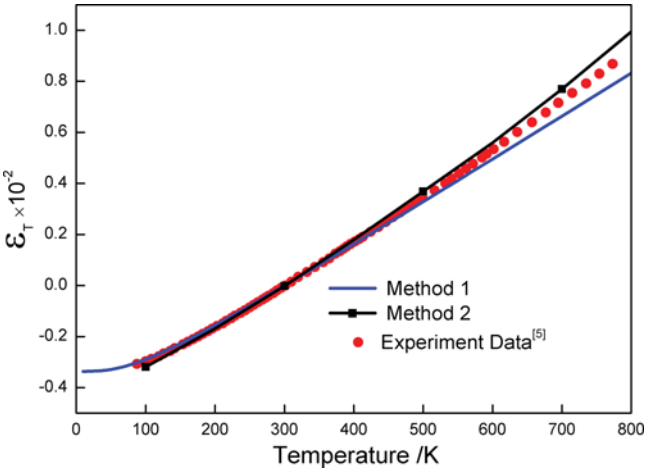

Figure 1 The thermal strain versus temperature for copper.

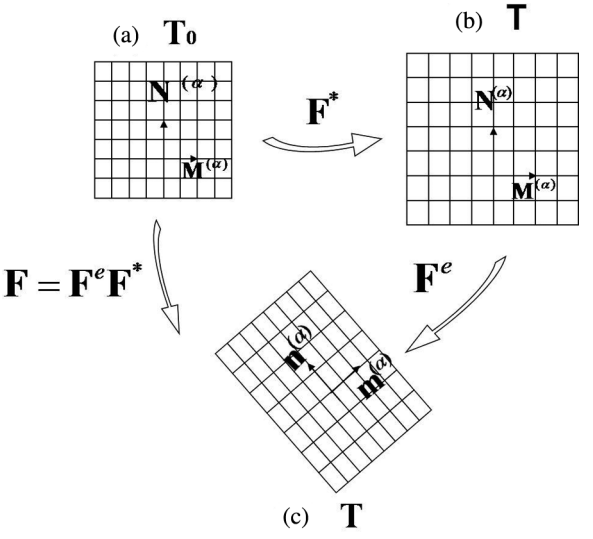

Figure 2 (a) Initial configuration; (b) Intermediate configuration; (c) Current configuration.

Figures 2(a)–(c) are the initial configuration, intermediate configuration and current configuration, respectively. The initial configuration in Figure 2(a) is at the state of undeformed crystal at room temperature T_0. The deformation gradient $\mathbf{F}^*$ is the free thermal expansion as the temperature rises from T_0 to T. As a result, the intermediate configuration Figure 2(b) is at the zero-stress state. $\mathbf{F}^e$ is the elastic deformation gradient from the intermediate configuration to the current configuration in Figure 2(c).

Downloaded by [University of Ottawa] at 01:45 11 June 2015

The total deformation gradient is

$$\mathbf{F} = \mathbf{F}^e\mathbf{F}^* \tag{9}$$

The second Piola–Kirchhoff stress [9, 25, 30] can be determined by

$$\mathbf{S} = \frac{\partial W}{\partial \mathbf{E}^e} = \frac{1}{V^*}\frac{\partial U_{tot}(\mathbf{E}^e)}{\partial \mathbf{E}^e} \tag{10}$$

The Cauchy stress is given by

$$\sigma = \frac{1}{V}\mathbf{F}^e\left\{\frac{\partial U_{tot}(\mathbf{E}^e)}{\partial \mathbf{E}^e}\right\}\mathbf{F}^{e^T} \tag{11}$$

Based on Eq. (9), the thermal strain tensor, elastic strain tensor and total strain tensor can be written respectively as

$$\mathbf{E}^* = (\mathbf{F}^{*T}\mathbf{F}^* - \mathbf{I})/2 \tag{12a}$$

$$\mathbf{E}^e = (\mathbf{F}^{eT}\mathbf{F}^e - \mathbf{I})/2 \tag{12b}$$

$$\mathbf{E} = (\mathbf{F}^T\mathbf{F} - \mathbf{I})/2 \tag{12c}$$

Substituting Eq. (9) into Eq. (12c), the Green strain tensor $\mathbf{E}$ can be expressed as

$$\begin{aligned}\mathbf{E} &= \frac{1}{2}[(\mathbf{F}^e\mathbf{F}^*)^T\mathbf{F}^e\ \mathbf{F}^* - \mathbf{I}]\\ &= \frac{1}{2}[\mathbf{F}^{*T}\ \mathbf{F}^{eT}\ \mathbf{F}^e\ \mathbf{F}^* - \mathbf{I}]\\ &= \frac{1}{2}[\mathbf{F}^{*T}(\mathbf{I} + 2\mathbf{E}^e)\ \mathbf{F}^* - \mathbf{I}]\\ &= \frac{1}{2}(\mathbf{F}^{*T}\mathbf{F}^* - \mathbf{I}) + \mathbf{F}^{*T}\ \mathbf{E}^e\ \mathbf{F}^*\\ &= \mathbf{E}^* + \mathbf{F}^{*T}\mathbf{E}^e\mathbf{F}^*\end{aligned} \tag{13}$$

Eq. (13) can be rewritten as

$$\mathbf{F}^{*^T}\mathbf{E}^e\mathbf{F}^* = \mathbf{E} - \mathbf{E}^* \tag{14}$$

Considering the Polar decomposition of the tensor, the deformation gradients $\mathbf{F}$, $\mathbf{F}^*$ and $\mathbf{F}^e$ can be rewritten respectively as

$$\begin{aligned}\mathbf{F} &= \mathbf{R}\mathbf{U}\\ \mathbf{F}^* &= \mathbf{R}^*\mathbf{U}^*\\ \mathbf{F}^e &= \mathbf{R}^e\mathbf{U}^e\end{aligned} \tag{15}$$

Downloaded by [University of Ottawa] at 01:45 11 June 2015

Without losing generality, one can assume $\mathrm{R}^* = \mathbf{I}$. Then Eq. (14) can be rewritten as

$$\mathbf{E}^e = (\mathbf{U}^*)^{-1}(\mathbf{E}-\mathbf{E}^*)(\mathbf{U}^*)^{-1} \tag{16}$$

Eq. (12a) can also be rewritten as

$$\mathbf{E}^* = [(\mathbf{U}^*)^2 - \mathbf{I}]/2 \tag{17}$$

Then the Taylor expansion of $\mathbf{U}^*$ is,

$$\mathbf{U}^* = (\mathbf{I} + 2\mathbf{E}^*)^{\frac{1}{2}} = \mathbf{I} + \mathbf{E}^* - \frac{1}{2}(\mathbf{E}^*)^2 + \cdots \tag{18}$$

If the thermal strain $\mathbf{E}^*$ is small, the following equations can be obtained,

$$\mathbf{U}^* \cong \mathbf{I} + \mathbf{E}^* \tag{19}$$

and

$$\mathbf{U}^* \cong \mathbf{I} \tag{20}$$

Substituting Eq. (20) into Eq. (16), the elastic Green strain tensor $\mathbf{E}^e$ can be expressed as

$$\mathbf{E}^e = \mathbf{E} - \mathbf{E}^* \tag{21}$$

Combining Eq. (11) with Eq. (21), the following equation can be obtained,

$$\sigma = \frac{1}{V}\mathbf{F}^e \left\{ \left[\frac{\partial U_{tot}(\mathbf{E}^e)}{\partial \mathbf{E}^e} \right]_{\mathbf{E}^e=\mathbf{E}-\mathbf{E}^*} \right\} \mathbf{F}^{e^T} \tag{22}$$

Eq. (22) is the new constitutive equation of thermoelasticity, and the thermal strain $\mathbf{E}^*$ is temperature dependent.

CALCULATION PROCEDURES

To verify the correction of the present constitutive Eq. (22) of thermoelasticity, a series of comparisons for calculated results should be carried out between the two thermal stress theories. The EAM potential proposed by Mishin et al. [33] for copper and Brenner potential for graphene [31, 34] are adopted in the following calculations.

For the previous thermal stress theory, the first step is to calculate vibration frequency ω_i of lattice. For copper and graphene, the frequency ω_i is obtained from Eqs. (A.5) and (B.6) with the Born-Karman boundary condition [25], respectively, then the stresses are obtained from Eq. (5) at the different loading paths, and the incremental loading is performed at specified temperature T. It is easy to note that the frequency ω_i varies with deformation.

Downloaded by [University of Ottawa] at 01:45 11 June 2015

For the present thermal stress theory, the first step is to determine the thermal strain $\mathbf{E}^*$, then calculate the stress from Eq. (22). As soon as the coefficient of thermal expansion is obtained, the thermal strain can be calculated from Eq. (6). The coefficient of thermal expansion could be obtained either from calculation [9, 26, 27] or from experiments [6]. For copper, the frequencies ω_i, the specific heat C_V and the coefficient of thermal expansion are calculated from Eq. (A.5), Eq. (A.6) and Eq. (A.7), respectively. For graphene, the frequencies ω_i, the specific heat C_V, the coefficients of thermal expansion and the thermal strain are calculated from Eq. (B.6), Eq. (B.7), Eqs. (B.9) and (B.10), and Eq. (B.13), respectively.

SIMULATION RESULTS AND DISCUSSION

The four different loading paths are performed at different temperatures. They are the uniaxial tension, pure shear and biaxial tension ($\varepsilon_{11} : \varepsilon_{22} = 1 : 2$ and $\varepsilon_{11} : \varepsilon_{22} = 1 : 3$), respectively. The stress-strain curves of copper are obtained at 300 K, 500 K and 800 K, and the stress-strain curves of graphene are calculated at 600 K, 1200 K and 1800 K.

Figure 3 shows the comparison of stress-strain curves for copper. Figures 3(a)–(f) are the results of uniaxial tension, pure shear, biaxial tensions ($\varepsilon_{11} : \varepsilon_{22} = 1 : 2$, $\varepsilon_{33} = \varepsilon_{22}$) and ($\varepsilon_{11} : \varepsilon_{22} = 1 : 3$, $\varepsilon_{33} = \varepsilon_{22}$) at 300 K, 500 K and 800 K, respectively. Similarly, Figure 4 shows the comparison of stress-strain curves for graphene. Figures 4 (a)–(f) are the results of uniaxial tension, pure shear, biaxial tensions ($\varepsilon_{11} : \varepsilon_{22} = 1 : 2$) and ($\varepsilon_{11} : \varepsilon_{22} = 1 : 3$) at 600 K, 1200 K and 1800 K, respectively. All calculated results of the current thermal stress theory are in good agreement with that of the theory based on quantum mechanics [9, 16, 27], which indicates that the present constitutive equation is correct.

For the previous theory, the normal vibration frequency should be computed from the force constant matrix, and the force constant matrix depends on the second-order derivative of the potential energy from Eqs. (A.1), (A.2) and (A.5). Therefore, the thermal stress depends on the accuracy of third-order derivative of the potential energy, it is a quite high demand to the interatomic potential. But for the new theory, the calculated result depends on the accuracy of the first-order derivative of the potential energy. Figures 3(c)–(f) show the curves of stress along x and y directions under biaxial load mode, as the strain increases, the little difference appears between the calculated results of two theories, which may be attributed to accuracy of the high order derivative of interatomic potential demanded by the previous theory.

The present constitutive Eq. (22) is quite compact and efficiency in comparison with the previous constitutive Eq. (5). There are several methods to get the thermal strain $\mathbf{E}^*$ either from experiment [5] or Eq. (8). The thermal strain $\mathbf{E}^*$ is only depended on temperature T. According to our new constitutive model, at the specified temperature T, the thermal strain $\mathbf{E}^*$ only need to be calculated once, however the stress tensor $\boldsymbol{\sigma}$ can be calculated from Eq. (22) for different applied strain, which is different from that of the previous theory.

However, the frequency ω_i and its derivative $\dfrac{\partial \omega_i}{\partial E}$ are dependent on the applied strain $\mathbf{E}$ in the previous constitutive Eq. (5). When the applied strain $\mathbf{E}$ increases or decreases, all of frequencies and their derivatives should be calculated repeatedly,

Downloaded by [University of Ottawa] at 01:45 11 June 2015

Downloaded by [University of Ottawa] at 01:45 11 June 2015

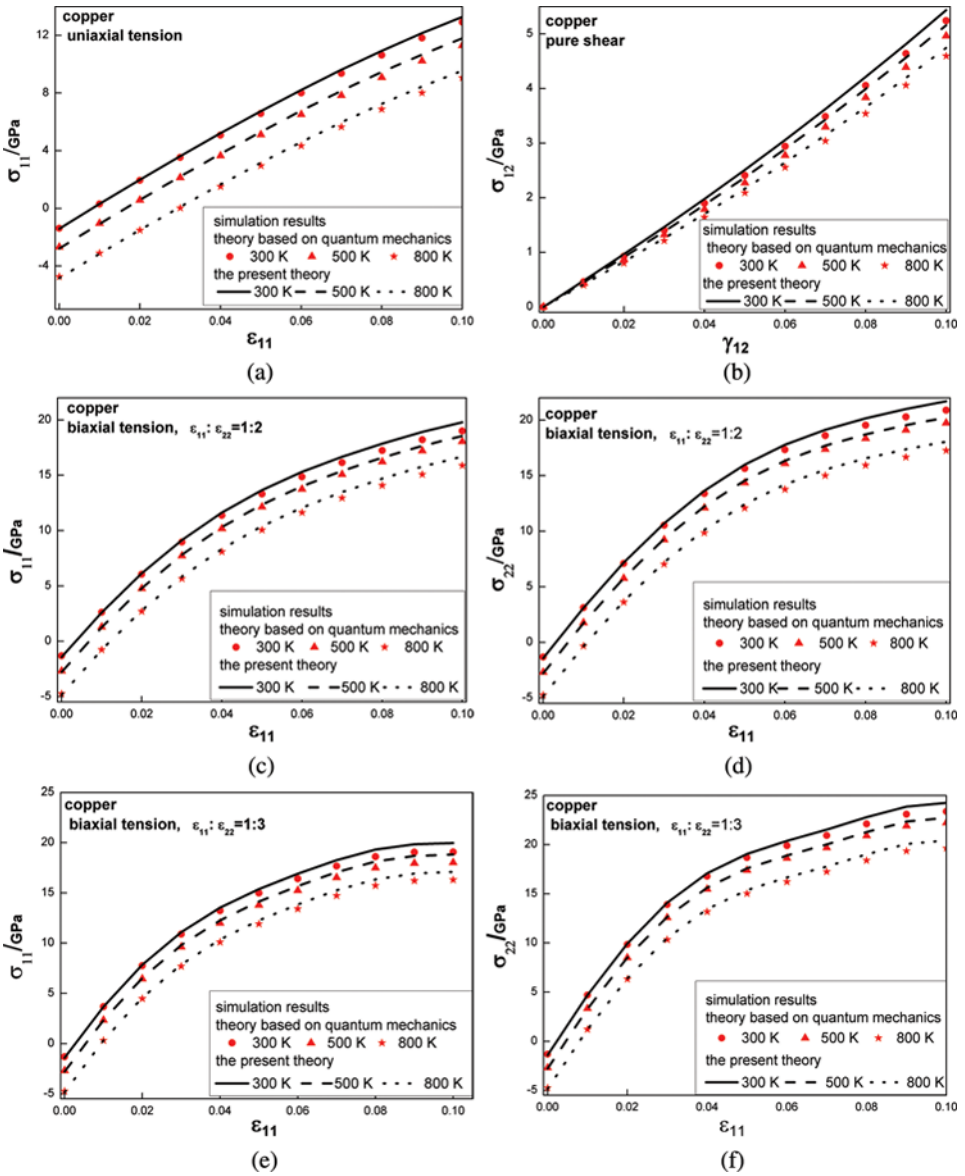

Figure 3 Comparison of simulation results in stress-strain curves between the present theory and the theory based on quantum mechanics for copper at 300 K, 500 K and 800 K. (a) Uniaxial tension; (b) pure shear; (c) biaxial tension, $\varepsilon_{11} : \varepsilon_{22} = 1 : 2, \varepsilon_{33} = \varepsilon_{22}$. Stress along x direction versus strain; (d) biaxial tension, $\varepsilon_{11} : \varepsilon_{22} = 1 : 2, \varepsilon_{33} = \varepsilon_{22}$. Stress along the y direction versus strain; (e) biaxial tension, $\varepsilon_{11} : \varepsilon_{22} = 1 : 3, \varepsilon_{33} = \varepsilon_{22}$. Stress along the x direction versus strain; (f) biaxial tension, $\varepsilon_{11} : \varepsilon_{22} = 1 : 3, \varepsilon_{33} = \varepsilon_{22}$. Stress along the y direction versus strain.

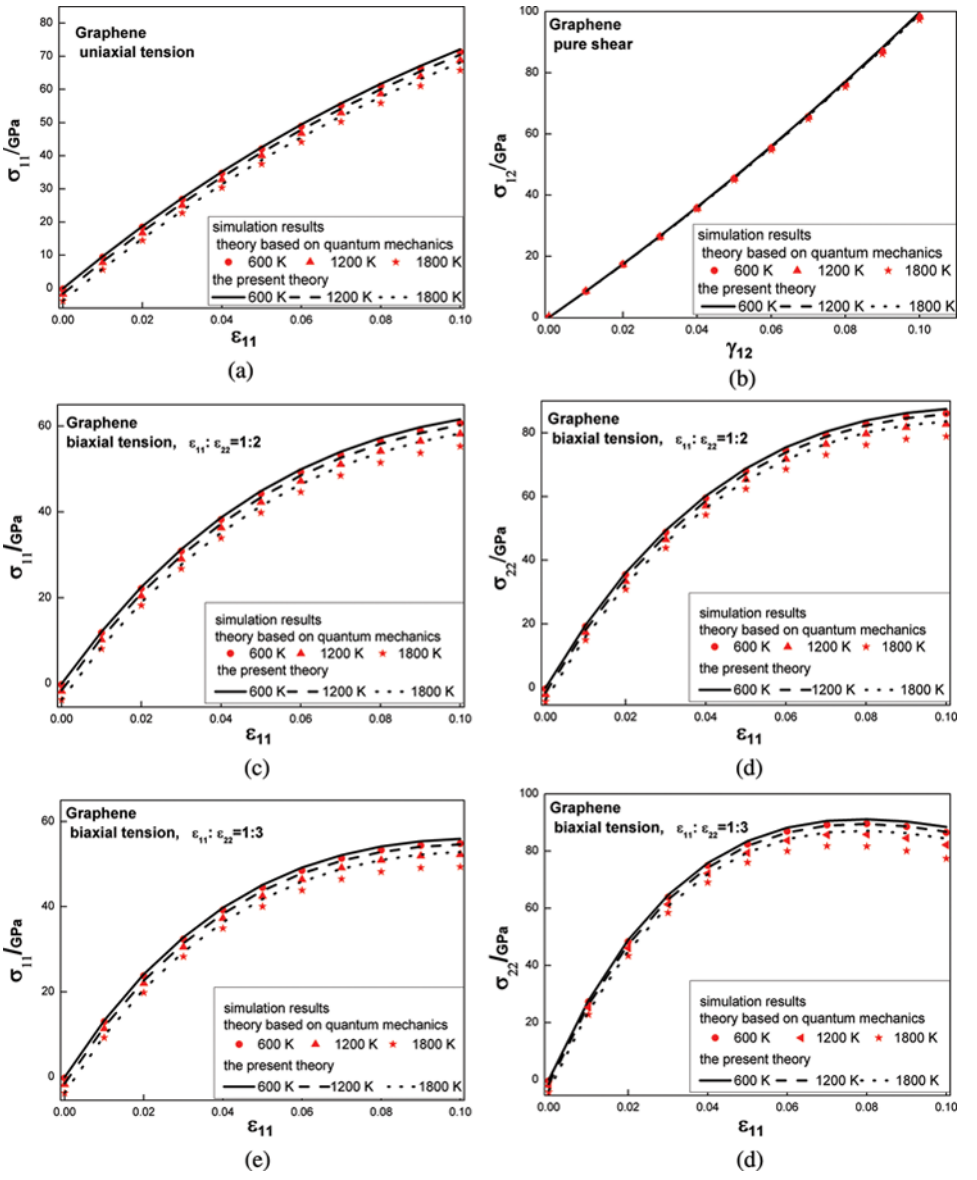

Figure 4 Comparison of simulation results in stress-strain curves between the present theory and the theory based on quantum mechanics for graphene at 600 K, 1200 K and 1800 K: (a) Uniaxial tension; (b) pure shear; (c) biaxial tension, $\varepsilon_{11} : \varepsilon_{22} = 1 : 2$. Stress along the x direction versus strain; (d) biaxial tension, $\varepsilon_{11} : \varepsilon_{22} = 1 : 2$. Stress along the y direction versus strain; (e) biaxial tension, $\varepsilon_{11} : \varepsilon_{22} = 1 : 3$. Stress along the x direction versus strain; (f) biaxial tension, $\varepsilon_{11} : \varepsilon_{22} = 1 : 3$. Stress along y direction versus strain.

costing more time. A comparison of the calculation efficiency has been carried out, the calculation speed of the new theory is about 30 times higher for copper and 60 times higher for grapheme than that of the previous theory due to its structure of non-Bravais lattice. The big difference of calculation efficiency between the two

Downloaded by [University of Ottawa] at 01:45 11 June 2015

thermal stress theories is attributed to that the terms ω_i and $\frac{\partial \omega_i}{\partial \mathbf{E}}$ need to be calculated repeatedly with deformation for the previous theory. Since the thermal strain is the intrinsic property of the materials, which does not depend on the applied strain, hence the Cauchy stress could be obtained directly by Eq. (22).

Another significance of the new theory of thermal stress is that it could be applied to different kinds of solid materials extensively. For amorphous materials, such as the metallic glass,it is difficult to calculate the frequencies of atoms, and it is quite difficult to obtain the theoretical prediction by using the previous thermal stress theory. However, if the thermal expanding coefficient and the thermal strain can be obtained from the experimental data and Eq. (6) respectively, the theoretical prediction of the thermal mechanical behavior could be calculated with the new thermoelasticity theory.

CONCLUSION

In this article, a constitutive equation of thermoelasticity for the solid materials is proposed. The thermal stresses are calculated for crystal copper and graphene under different loading paths at different temperatures. The calculated results are in good agreement with those of the previous constitutive equation of thermoelasticity based on quantum mechanics at the different temperatures. A lot of comparisons also show that the present theory is more concise and efficient in comparison with the previous thermal stress theory in the practical applications.

APPENDIX A

A.1. Vibration Frequencies of Copper

The force acting on atom i is equal to

$$\begin{aligned} \boldsymbol{f}_i &= -\frac{\partial U_{tot}}{\partial \boldsymbol{r}_i} = -\sum_{j\in\Omega_i} \frac{\partial U_{tot}}{\partial r_{ij}} \frac{\partial \boldsymbol{r}_{ij}}{\partial \boldsymbol{r}_i} = \sum_{j\in\Omega_i} f_{ij}\boldsymbol{e}_{ij} \\ \boldsymbol{e}_{ij} &= \frac{\boldsymbol{r}_{ij}}{\boldsymbol{r}_{ij}} \quad f_{ij} = \frac{\partial U_{tot}}{\partial \boldsymbol{r}_{ij}} \end{aligned} \tag{A.1}$$

The dynamic equation of atom k is given by Tang et al. [32]

$$\begin{aligned} m_k \ddot{\boldsymbol{u}}_k &= \sum_{j\in\Omega_k} \boldsymbol{K}_{kj} \bullet (\boldsymbol{u}_j - \boldsymbol{u}_k) \\ \boldsymbol{K}_{kj} &= \frac{f_{kj}(r_{kj})}{r_{kj}}\boldsymbol{I} + (f'_{kj}(r_{kj}) - \frac{f_{kj}(r_{kj})}{r_{kj}})\boldsymbol{e}_{kj} \otimes \boldsymbol{e}_{kj} \end{aligned} \tag{A.2}$$

where $\boldsymbol{u}_j$ is the displacement of atom j, $\boldsymbol{I}$ is the second-order unit tensor, and $\otimes$ is the tensor multiplication operator.

Equation (A.2) can be solved as

$$\boldsymbol{u}_j = \boldsymbol{A}_j e^{i(\omega t - \boldsymbol{r}_j \bullet \boldsymbol{q})} \tag{A.3}$$

Downloaded by [University of Ottawa] at 01:45 11 June 2015

A calculation system of parallelepiped cells is selected in this study, and the size of the simulation cell is $N_1\boldsymbol{a}_1$, $N_2\boldsymbol{a}_2$ and $N_3\boldsymbol{a}_3$, respectively, where $\boldsymbol{a}_1$, $\boldsymbol{a}_2$ and $\boldsymbol{a}_3$ are the three basis vectors of Bravais lattice, and N_1, N_2 and N_3 are integers. The Born–Karman boundary condition [25] is applied.

Substituting Eq. (A.3) into Eq. (A.2),

$$-m_k\boldsymbol{A}_k\omega^2 = \sum_{j\in\Omega_k}\boldsymbol{K}_{kj}\bullet(\boldsymbol{A}_j e^{-i\boldsymbol{r}_{kj}\bullet\boldsymbol{q}} - \boldsymbol{A}_k)\quad k = 1,\ldots,N \tag{A.4}$$

where N is the total number of atoms in the system.

For copper, per unit cell contains only one atom. All atoms have the same magnitude, $\boldsymbol{A}_k = \boldsymbol{A}_j = \boldsymbol{A}$.

As a result, each copper atom interacts with 54 neighbors, which include the nearest neighbors, second nearest neighbors up to fourth-nearest neighbors.

Hence for atom k the characteristic equation can be written as

$$\left|m\omega^2\boldsymbol{I} + \sum_{j=1}^{54}\boldsymbol{K}_{kj}\bullet(\boldsymbol{e}^{-i\boldsymbol{r}_{kj}\bullet\boldsymbol{q}} - 1)\right| = 0 \tag{A.5}$$

In order to obtain valuable results, the EAM potential proposed by Mishin et al. [26] for copper is adopted in this article.

A.2. Specific Heat and Coefficient of Thermal Expansion

The specific heat C_V is given in [27],

$$\begin{aligned}\overline{E} &= \sum_q\sum_{s=1}^{3}\left(\frac{1}{2}\hbar\omega_s(\boldsymbol{q}) + \frac{\hbar\omega_s(\boldsymbol{q})}{e^{\hbar\omega_s(\boldsymbol{q})/k_BT}-1}\right)\\ C_V &= \frac{d\overline{E}(T)}{dT} = \sum_q\sum_{s=1}^{3}k_B\frac{(\hbar\omega_s(\boldsymbol{q})/k_BT)^2\,e^{\hbar\omega_s(\boldsymbol{q})/k_BT}}{(e^{\hbar\omega_s(q)/k_BT}-1)^2}\end{aligned} \tag{A.6}$$

where $\omega_s(\boldsymbol{q})$ is the vibration frequency of the crystal lattice. The bulk modulus of crystal can be calculated by $K_0 = V_0\left(\frac{d^2U_{tot}}{dV^2}\right)_{V_0}$. Where, V_0 is the volume prior to deformation and U_{tot} is the total potential energy. The calculation result is $K_0 = 138$ GPa, which is in good agreement with experimental data 137 GPa [29].

According to the Grüneisen's law, the coefficient of thermal expansion α of copper is given by

$$\alpha = \frac{1}{3}\alpha_V = \frac{\gamma}{3K_0}\frac{C_V}{V} \tag{A.7}$$

For copper, γ is a constant and taken to be 2.0.

The thermal strain is given by

$$\varepsilon_T = \int_{T_0}^{T}\alpha dT \tag{A.8}$$

which is the same as Eq. (6) in main text.

Downloaded by [University of Ottawa] at 01:45 11 June 2015

Downloaded by [University of Ottawa] at 01:45 11 June 2015

APPENDIX B

B.1. Vibration Frequencies of Graphite

For graphite, the interlayer interaction is van der waals force which is quite small compared to the in-plane interaction. As a result, the interlayer interaction could be neglected in the dynamic equation of the carbon atom. Therefore graphene can be a substitute for graphite when the vibration frequencies of the system are calculated.

As is shown in Figure 5, carbon atoms in graphene can be classified into two types A and B.

For a two-dimensional graphene crystal, wave vector q can be expressed as

$$\boldsymbol{q} = \frac{k_1}{N_1}\boldsymbol{b}_1 + \frac{k_2}{N_2}\boldsymbol{b}_2, \quad k_1 = 1, \ldots, N_1, \quad k_2 = 1, \ldots, N_2 \tag{B.1}$$

where $\boldsymbol{b}_1$ and $\boldsymbol{b}_2$ are the basis vector of the reciprocal lattice.

The cut-off function of carbon's Brenner potential [31, 34] can be written as

$$f_C\left(r_{ij}\right) = \begin{cases} 1 & r < R^{(1)} \\ \frac{1}{2}\left\{1 + \cos\left[\pi\left(r - R^{(1)}\right) / \left(R^{(2)} - R^{(1)}\right)\right]\right\} & R^{(1)} < r < R^{(2)} \\ 0 & r > R^{(2)} \end{cases} \tag{B.2}$$

where $R^{(1)} = 0.17nm$, $R^{(2)} = 0.2nm$. As a result, for one carbon atom A, it interacts with 3 nearest neighbors B. The dynamic equations therefore can be expressed by

$$\begin{aligned} m\ddot{\boldsymbol{u}}_{A_i} &= \sum_{j=1}^{3} K(r_{A_iB_j}) \bullet (u_{B_j} - u_{A_i}) \\ m\ddot{\boldsymbol{u}}_{B_i} &= \sum_{j=1}^{3} K(r_{B_iA_j}) \bullet (u_{A_j} - u_{B_i}) \end{aligned} \tag{B.3}$$

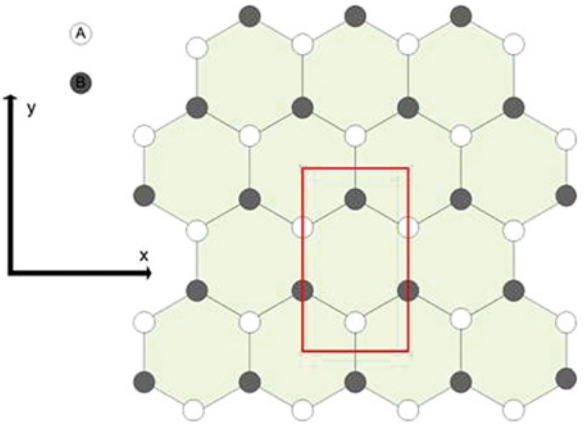

Figure 5 A schematic diagram of the atomic structure of a graphene with a representative atoms. The open circles represent the carbon atom A, and the shaded circles represent the carbon atom B.

where A and B represent the two types of the atom, and i and j are serial numbers of the atoms.

In graphene, A and B atoms have different amplitudes. The solutions of lattice wave are

$$\begin{aligned} \boldsymbol{u}_{A_i} &= \boldsymbol{A} e^{i\left(\omega t - \boldsymbol{r}_{A_i} \bullet q\right)} \\ \boldsymbol{u}_{B_i} &= \boldsymbol{B} e^{i\left(\omega t - \boldsymbol{r}_{B_i} \bullet q\right)} \end{aligned} \tag{B.4}$$

Substituting Eq. (B.4) into Eq. (B.3), we get

$$\left(m\omega^2 \boldsymbol{I} - \boldsymbol{J}\right)\left(A_x, A_y, A_z, B_x, B_y, B_z\right)^T = \boldsymbol{0} \tag{B.5}$$

where $\boldsymbol{J}$ is a 6×6 matrix, and A_x, A_y, A_z, B_x, B_y, and B_z are the components of the amplitudes of the atoms.

The characteristic equation can be written as

$$\left|m\omega^2 \boldsymbol{I} - \boldsymbol{J}\right| = 0 \tag{B.6}$$

Hence six vibration frequencies can be obtained for each $\boldsymbol{q}$.

B.2. Specific Heat and Coefficient of Thermal Expansion of Graphite

The C_V for graphite can be composed of two components [34]:

$$C_V = \frac{2}{3} C_{V,a} + \frac{1}{3} C_{V,c} \tag{B.7}$$

where $C_{V,a}$ is the in-plane specific heat at constant volume, $C_{V,c}$ is the out-of-plane specific heat at constant volume. $C_{V,a}$ and $C_{V,c}$ take the forms

$$\begin{aligned} C_{V,a} &= \sum_q \sum_{s=1}^{4} k_B \frac{\left(\hbar\omega_s^a(\boldsymbol{q})/k_B T\right)^2 e^{\hbar\omega_s^a(q)/k_B T}}{\left(e^{\hbar\omega_s^a(q)/k_B T} - 1\right)^2} \\ C_{V,c} &= \sum_q \sum_{s=5}^{6} k_B \frac{\left(\hbar\omega_s^c(\boldsymbol{q})/k_B T\right)^2 e^{\hbar\omega_s^c(q)/k_B T}}{\left(e^{\hbar\omega_s^c(q)/k_B T} - 1\right)^2} \end{aligned} \tag{B.8}$$

where $\omega_s^a(\boldsymbol{q})$ is the in-plane frequency, $\omega_s^c(\boldsymbol{q})$ is the out-of-plane frequency.

Since thermal expansion of graphite is anisotropic, the expression of Grüneisen's law for graphite is different from that for copper. As pointed by Morgan [34], in-plane CTE and out-of-plane CTE are the functions of $C_{V,a}$ and $C_{V,c}$:

$$\alpha_a = \frac{\gamma_a}{V}\left(S_{11} + S_{12}\right)\frac{2}{3} C_{V,a} + \frac{\gamma_c}{V} S_{13} \frac{1}{3} C_{V,c} + CT \tag{B.9}$$

$$\alpha_c = \frac{\gamma_a}{V}\left(S_{31} + S_{32}\right)\frac{2}{3} C_{V,a} + \frac{\gamma_c}{V} S_{33} \frac{1}{3} C_{V,c} + NT \tag{B.9}$$

Downloaded by [University of Ottawa] at 01:45 11 June 2015

where S_{11}, S_{12}, S_{13} and S_{33} are the elastic flexibility coefficients of the crystal; C and N are the parameters; V is the mole volume and is equal to 5.31 $cm^3/mole$; We set $\gamma_a = 2.05$ and α_a as the in-plane and out-of-plane Grüneisen parameters, respectively.

According to references [34, 35], at room temperature, we have

$$\begin{aligned} S_{11} + S_{12} &= 1.05 \times 10^{-13} cm^2/dyn \\ S_{13} &= -2.49 \times 10^{-13} cm^2/dyn \\ S_{33} &= 26.3 \times 10^{-13} cm^2/dyn \end{aligned} \tag{B.11}$$

B.3. Lattice Spacing of Graphite

Since the CTE of graphite in a-direction and c-direction are different, the a-spacing and c-spacing of graphite are also different, which can be expressed as the functions of α_a and α_c, respectively:

$$\begin{aligned} a(T) &= a_0(1 + \int_0^T \alpha_a dt) \\ c(T) &= c_0(1 + \int_0^T \alpha_c dt) \end{aligned} \tag{B.12}$$

where, $a_0 = 0.24618nm$, $c_0 = 0.66818nm$ [35], and they are lattice a-spacing and lattice c-spacing at absolute zero temperature, respectively.

B.4. The Thermal Strain of Graphite

From Eq. (B.12), one can obtain the thermal strain in a-direction $\varepsilon_a(T)$ and the thermal strain in c-direction $\varepsilon_c(T)$ as follows

$$\begin{aligned} \varepsilon_a(T) &= \frac{a - a_0}{a_0} = \int_0^T \alpha_a dT \\ \varepsilon_c(T) &= \frac{c - c_0}{c_0} = \int_0^T \alpha_c dT \end{aligned} \tag{B.13}$$

Then the thermal strain tensor $\mathbf{E}^*$ for graphite can be expressed as

$$\mathbf{E}^*(T) = \begin{bmatrix} \varepsilon_a(T) & 0 & 0 \\ 0 & \varepsilon_a(T) & 0 \\ 0 & 0 & \varepsilon_c(T) \end{bmatrix} \tag{B.14}$$

NOMENCLATURE

A	Helmholtz free energy
$\hbar$	Planck constant
k_B	Boltzmann constant

Downloaded by [University of Ottawa] at 01:45 11 June 2015

U_{tot}	Total potential energy of the system
W	Strain energy density
$\mathbf{F}$	Deformation gradient
$\mathbf{F}^e$	Elastic deformation gradient
ω_j	Thermal deformation gradient
R	Rotation tensors
$\mathbf{R}^*$	Thermal rotation tensors
$\mathbf{R}^e$	Elastic rotation tensors
$\mathbf{U}$	Stretch tensors
$\mathbf{U}^*$	Thermal stretch tensors
$\mathbf{U}^e$	Elastic stretch tensors
$\mathbf{E}$	Green strain tensor
$\mathbf{E}^e$	Elastic Green strain tensor
$\mathbf{E}^*$	Thermal strain tensor
$\mathbf{S}$	Second Piola-Kirchhoff stress
ω_i	Frequency of the i*th* normal vibration mode
$\bar{E}_i$	Thermo energy
$\boldsymbol{\sigma}$	Cauchy stress
V_0	Volume at the initial configuration
V^*	Volume at the intermediate configuration
V	Volume at the current configuration
ε_T	Thermal strain
$r^{(0)}(T)$	Lattice constant
e_{ij}	Unit vector from atom i to atom j
r_{kj}	Bond length between atom i and atom j
Ω_i	Set of all atoms which interact with the atom i
f_{ij}	Interaction force between atom i and atom j
u_j	Displacement of atom j
$\otimes$	Tensor multiplication operator
C_V	Specific heat
$\overline{E}$	Total thermal energy
γ	Grüneisen's parameter
K_0	Bulk modulus of the crystal

Downloaded by [University of Ottawa] at 01:45 11 June 2015

FUNDING

This work is supported by the National Natural Science Foundation of China (Grant nos. 11021262, 11172303, 11132011) and National Basic Research Program of China through Grant no. 2012CB937500.

REFERENCES

1. S. D. Senturia, *Microsystem Design*, Kluwer, New York, 2000.
2. J. R. Neighbours and G. A. Alers. Elastic Constants of Silver and Gold, *Physical Review,* vol. 113, pp. 707, 1958.
3. W. B. Daniels and C. S. Smith, Pressure Derivatives of the Elastic Constants of Copper, Silver, and Gold to 10000 Bars, *Physical Review*, vol. 111, pp. 713, 1958.

4. D. E. Gray, *American Institute of Physics Handbook*, 2nd ed., McGraw-Hill, New York, 1963.
5. F. C. Nix and D. MacNair, The Thermal Expansion of Pure Metals Copper, Gold, Aluminum, Nickel, and Iron, *Physical Review*, vol. 60, pp. 597–605, 1941.
6. B. H. Billings and D. E. Gray, *American Institute of Physics Handbook 1972*, McGraw-Hill, New York, 1972.
7. A. S. Khan and S. Yu, Deformation Induced Anisotropic Responses of Ti–6Al–4V Alloy. Part I: Experiments, *International Journal of Plastics*, vol. 38, pp. 1–13, 2012.
8. A. S. Khan, S. Yu, and H. Liu, Deformation Induced Anisotropic Responses of Ti–6Al–4V Alloy Part II: A Strain Rate and Temperature Dependent Anisotropic Yield Criterion, *International Journal of Plastics*, vol. 38, pp. 14–26, 2012.
9. H. Jiang, Y. Huang, and K. C. Hwang, A Finite-Temperature Continuum Theory Based on Inter-Atomic Potentials, *Journal of Engineering Material Technology*, vol. 127, pp. 408–416, 2005.
10. M. Zhou, Thermomechanical Continuum Representation of Atomistic Deformation at Arbitrary Size Scales, *Proceedings of the Royal Society A,* vol. 461, pp. 3437–3472, 2005.
11. W. K. Liu, E. G. Karpov, and H. S Park, *Nano-Mechanics and Materials Theory, Multiscale Methods and Applications,* Wiley, New York, 2005.
12. D. Frenkel and B. Smit, *Understanding Molecular Simulation: From Algorithms to Applications,* 2nd ed., Academic Press, San Diego, California, 2002.
13. E. G. Karpov, H. S. Park, and W. K. Liu, A Phonon Heat Bath Approach for the Atomistic and Multiscale Simulation of Solids, *International Journal of Numerical Methods Engineering*, vol. 70, pp. 351–378, 2007.
14. L. E. Shilkrot, W. A. Curtin, and R. E. Miller, A Coupled Atomistic/Continuum Model of Defects in Solids, *Journal of Mechanical Physical Solids*, vol. 50, pp. 2085–2106, 2002.
15. J. Fish and W. Chen, Discrete-to-Continuum Bridging Based on Multigrid Principles, *Computation Methods Applied Mechanical Engineering*, vol. 193, pp. 1693–1711, 2004.
16. A. To, W. Liu, and A. Kopacz, A Finite Temperature Continuum Theory Based on Interatomic Potential in Crystalline Solids, *Computational Mechanics*, vol. 42, p. 531, 2008.
17. P. Zhang, Y. G. Huang, P. H. Geubelle, and K. C. Hwang, On the Continuum Modeling of Carbon Nanotubes, *Acta Mechanica Sinica*, vol. 18, p. 528, 2002.
18. E. B. Tadmor, M. Ortiz, and R. Phillips, Quasicontinuum Analysis of Defects in Solids, *Philosophical Magazine A*, vol. 73, pp. 1529 –1563, 1996.
19. E. B. Tadmor, G. S. Smith, N. Bernstein, and E. Kaxiras, Mixed Finite Element and Atomistic Formulation for Complex Crystals, *Physical Review B*, vol. 59, p. 235, 1999.
20. V. B. Shenoy, R. Miller, E. B. Tadmor, D. Rodney, R. Phillips, and M. Ortiz, An Adaptive Finite Element Approach to Atomic-Scale Mechanics—The Quasicontinuum Method*, Journal of Mechanical Physical Solids*, vol. 47, pp. 611–642, 1999.
21. E. B. Tadmor and R. E. Miller, *Modeling Materials: Continuum, Atomistic and Multiscale Techniques*, Cambridge University Press, Cambridge, UK, 2011.
22. V. B. Shenoy and R. Phillips, Finite Temperature Quasicontinuum Methods, *Materials Research Society,* vol. 538, pp. 465–472, 1999.
23. R. Miller and E. B. Tadmor, The Quasicontinuum Method: Overview, Applications and Current Directions,*Journal of Computer-Aided Material Design,* vol. 9, pp. 203–239, 2002.
24. L. M. Dupuy, E. B. Tadmor, R. E. Miller, and R. Phillips, Finite-Temperature Quasicontinuum: Molecular Dynamics Without All the Atoms, *Physical Review Letters*, vol. 95, pp. 060202, 2005.

Downloaded by [University of Ottawa] at 01:45 11 June 2015

25. Z. Tang and N. R. Aluru, Multiscale Mechanical Analysis of Silicon Nanostructures by Combined Finite Temperature Models, *Computational Methods in Applied Mechanical Engineering,* vol. 197, pp. 3215–3224, 2008.
26. Z. Tang, H. Zhao, G. Li, and N. R. Aluru, Finite-Temperature Quasicontinuum Method for Multiscale Analysis of Silicon Nanostructures, *Physical Review B,* vol. 74, pp. 064110, 2006.
27. H. Zhao, Z. Tang, G. Li, and .N. R. Aluru, Quasiharmonic Models for the Calculation of Thermodynamic Properties of Crystalline Silicon under Strain, *Journal of Applied Physics*, vol. 99, pp. 064314, 2006.
28. M. Born and K. Huang, *Dynamical Theory of the Crystal Lattices*, Oxford University Press, Oxford, UK, 1954.
29. F. Milstein, Theoretical Elastic Behavior of Crystals at Large Strains, *Journal of Material Science,* vol. 15, pp. 1071–1084, 1980.
30. R. Hill, Aspects of Invariance in Solid Mechanics, *Advances in Applied Mechanics*, vol. 18, pp. 1–75, 1978.
31. F. Liu, Q. H. Tang, B. S. Shang, and T. C. Wang, Simple Optimized Brenner Potential for Thermodynamic Properties of Diamond, *Philosophical Magazine*, vol. 92, pp. 500–515, 2012.
32. Q. H. Tang, T. C. Wang, B. S. Shang, and F. Liu, Thermodynamic Properties and Constitutive Relations of Crystals at Finite Temperature, *Science China G.,* vol. 55, pp. 918–926, 2012.
33. Y. Mishin, M. Mehl, and D. Papaconstantopoulos, Structural Stability and Lattice Defects in Copper: Ab initio, Tight-Binding, and embedded-atom calculations, *Physical Review B*, vol. 63, pp. 224106, 2001.
34. D.W. Brenner, Empirical Potential for Hydrocarbons for Use in Simulating the Chemical Vapor Deposition of Diamond Films, *Physical Review B*, vol. 42, pp. 9458, 1990.
35. W. C. Morgan, Thermal-Expansion Coefficients of Graphite Crystals, *Carbon*, vol. 10, p. 73, 1972.

Downloaded by [University of Ottawa] at 01:45 11 June 2015